

# Fabry-Perot cavity based on silica tube for strain sensing at high temperatures

Marta S. Ferreira,<sup>1,2,\*</sup> Paulo Roriz,<sup>1</sup> Jörg Bierlich,<sup>3</sup> Jens Kobelke,<sup>3</sup> Katrin Wondraczek,<sup>3</sup>  
Claudia Aichele,<sup>3</sup> Kay Schuster,<sup>3</sup> José L. Santos,<sup>1,2</sup> and Orlando Frazão<sup>1,2</sup>

<sup>1</sup>INESC Porto, Rua do Campo Alegre 687, 4169-007 Porto, Portugal

<sup>2</sup>Faculdade de Ciências da Universidade do Porto, Rua do Campo Alegre 687, 4169-007 Porto, Portugal

<sup>3</sup>Leibniz Institute of Photonic Technology, Albert-Einstein-Straße 9, 07745 Jena, Germany

\*msaf@inescporto.pt

**Abstract:** In this work, a Fabry-Perot cavity based on a new silica tube design is proposed. The tube presents a cladding with a thickness of  $\sim 14$   $\mu\text{m}$  and a hollow core. The presence of four small rods, of  $\sim 20$   $\mu\text{m}$  diameter each, placed in diametrically opposite positions ensure the mechanical stability of the tube. The cavity, formed by splicing a section of the silica tube between two sections of single mode fiber, is characterized in strain and temperature (from room temperature to 900 °C). When the sensor is exposed to high temperatures, there is a change in the response to strain. The influence of the thermal annealing is investigated in order to improve the sensing head performance.

©2015 Optical Society of America

**OCIS codes:** (060.0060) Fiber optics and optical communications; (060.2370) Fiber optics sensors; (120.2230) Fabry-Perot.

---

## References and links

1. Y. Chen and H. F. Taylor, "Multiplexed fiber Fabry-Perot temperature sensor system using white-light interferometry," *Opt. Lett.* **27**(11), 903–905 (2002).
2. L.-C. Xu, M. Deng, D.-W. Duan, W.-P. Wen, and M. Han, "High-temperature measurement by using a PCF-based Fabry-Perot interferometer," *Opt. Lasers Eng.* **50**(10), 1391–1396 (2012).
3. M. S. Ferreira, L. Coelho, K. Schuster, J. Kobelke, J. L. Santos, and O. Frazão, "Fabry-Perot cavity based on a diaphragm-free hollow-core silica tube," *Opt. Lett.* **36**(20), 4029–4031 (2011).
4. H. Y. Choi, K. S. Park, S. J. Park, U.-C. Paek, B. H. Lee, and E. S. Choi, "Miniature fiber-optic high temperature sensor based on a hybrid structured Fabry-Perot interferometer," *Opt. Lett.* **33**(21), 2455–2457 (2008).
5. H. Y. Choi, G. Mudhana, K. S. Park, U.-C. Paek, and B. H. Lee, "Cross-talk free and ultra-compact fiber optic sensor for simultaneous measurement of temperature and refractive index," *Opt. Express* **18**(1), 141–149 (2010).
6. D. W. Duan, Y. J. Rao, W. P. Wen, J. Yao, D. Wu, L. C. Xu, and T. Zhu, "In-line all-fibre Fabry-Pérot interferometer high temperature sensor formed by large lateral offset splicing," *Electron. Lett.* **47**(6), 401–403 (2011).
7. J.-L. Kou, J. Feng, L. Ye, F. Xu, and Y.-Q. Lu, "Miniaturized fiber taper reflective interferometer for high temperature measurement," *Opt. Express* **18**(13), 14245–14250 (2010).
8. T. Wei, Y. Han, H.-L. Tsai, and H. Xiao, "Miniaturized fiber inline Fabry-Perot interferometer fabricated with a femtosecond laser," *Opt. Lett.* **33**(6), 536–538 (2008).
9. Y. J. Rao, T. Zhu, X. C. Yang, and D. W. Duan, "In-line fiber-optic etalon formed by hollow-core photonic crystal fiber," *Opt. Lett.* **32**(18), 2662–2664 (2007).
10. P. A. R. Tafalo, P. A. S. Jorge, J. L. Santos, and O. Frazão, "Fabry-Pérot cavities based on chemical etching for high temperature and strain measurement," *Opt. Commun.* **285**(6), 1159–1162 (2012).
11. S. Liu, Y. Wang, C. Liao, G. Wang, Z. Li, Q. Wang, J. Zhou, K. Yang, X. Zhong, J. Zhao, and J. Tang, "High-sensitivity strain sensor based on in-fiber improved Fabry-Perot interferometer," *Opt. Lett.* **39**(7), 2121–2124 (2014).
12. F. C. Favero, L. Araujo, G. Bouwmans, V. Finazzi, J. Villatoro, and V. Pruneri, "Spheroidal Fabry-Perot microcavities in optical fibers for high-sensitivity sensing," *Opt. Express* **20**(7), 7112–7118 (2012).
13. J. Villatoro, V. Finazzi, G. Coviello, and V. Pruneri, "Photonic-crystal-fiber-enabled micro-Fabry-Perot interferometer," *Opt. Lett.* **34**(16), 2441–2443 (2009).
14. D.-W. Duan, Y.-J. Rao, Y.-S. Hou, and T. Zhu, "Microbubble based fiber-optic Fabry-Perot interferometer formed by fusion splicing single-mode fibers for strain measurement," *Appl. Opt.* **51**(8), 1033–1036 (2012).

15. Z. L. Ran, Y. J. Rao, H. Y. Deng, and X. Liao, "Miniature in-line photonic crystal fiber etalon fabricated by 157 nm laser micromachining," *Opt. Lett.* **32**(21), 3071–3073 (2007).
16. M. Deng, C.-P. Tang, T. Zhu, and Y.-J. Rao, "PCF-based Fabry-Pérot interferometric sensor for strain measurement at high temperatures," *IEEE Photon. Technol. Lett.* **23**(11), 700–702 (2011).
17. K. Schuster, S. Unger, C. Aichele, F. Lindner, S. Grimm, D. Litzkendorf, J. Kobelke, J. Bierlich, K. Wondraczek, and H. Bartelt, "Material and technology trends in fiber optics," *Adv. Opt. Technol.* **3**(4), 447–468 (2014).
18. M. S. Ferreira, J. Bierlich, J. Kobelke, K. Schuster, J. L. Santos, and O. Frazão, "Towards the control of highly sensitive Fabry-Pérot strain sensor based on hollow-core ring photonic crystal fiber," *Opt. Express* **20**(20), 21946–21952 (2012).
19. O. Mazurin, M. Streltsina, and T. Shvaiko-Shvaikovskaia, "Handbook of glass data. Part A: silica glass and binary silicate glasses," **15** (1983).
20. J. A. Bucaro and H. D. Dardy, "High-temperature Brillouin scattering in fused quartz," *J. Appl. Phys.* **45**(12), 5324–5329 (1974).

---

## 1. Introduction

Optical fiber sensors based on Fabry-Perot (FP) cavities, due to their inherent characteristics, are suitable for many different applications, such as in sensing of physical, chemical and biological parameters. These structures are easy to produce, are compact and reliable. Besides, the simple configuration ensures stability and ability to be multiplexed [1].

The measurement of physical parameters such as strain and temperature is of most importance in practical applications, in particular when extreme conditions are involved. Many different FP based configurations have been proposed where temperatures up to 1100 °C have been tested [2]. In order to obtain FP based sensors more sensitive to temperature, the cavity is usually formed at the tip of the fiber. These structures can be created by fusion splicing different types of fibers [3–5], by splicing two sections of single mode fiber (SMF) with a large lateral offset [6], or even by fabricating a FP modal interferometer in a fiber taper probe [7]. These configurations usually present reduced dimensions, of the order of hundreds of micrometers. When the FP cavities are formed between two sections of fiber, they become less sensitive to temperature, with sensitivities lower than 1 pm/°C. The structures can be formed by femtosecond laser ablation [8], by splicing a short section of hollow core photonic crystal fiber [9] or a chemically etched multimode fiber section [10] between two sections of SMF. Another possibility is to form an air cavity, like a bubble or a spheroidal cavity, inside the fiber. There are different ways to fabricate the structures through splicing. For example, the splice of two sections of SMF [11,12], SMF spliced to index guiding photonic crystal fiber [13] or splicing a flat and hemispherical tip of SMF [14]. Due to their configuration and low thermal sensitivity, these FP cavities become highly attractive to measure other parameters such as strain. However, the sensors proposed in these works were characterized to strain and temperature separately.

The measurement of strain at high temperatures using FP cavities was proposed by Ran *et al* in 2007 [15]. An etalon in photonic crystal fiber was fabricated using 157 nm laser micromachining. Strain measurements were carried out over temperatures as high as 800 °C. The fabrication of an air bubble cavity by splicing a multimode photonic crystal fiber to a SMF has also been proposed [16]. In this case, strain measurements up to 1850  $\mu\epsilon$  were performed in a temperature range between 100 °C to 750 °C.

In this work, a Fabry-Perot cavity based on a new silica tube design is proposed. A number of sensors are fabricated and tested to strain and temperatures as high as 900 °C. Given the low temperature sensitivity, this configuration is also subjected to strain at different temperatures. Besides, the effect of the annealing is also analyzed. The proposed sensor exhibits features that translate into a different solution for the measurement of strain in harsh environments.

## 2. Experimental results

All components of the silica tube used in this work were manufactured from high purity silica Heraeus Suprasil® F300. The first procedure was to define the sintering of the four rods (diameter 1.2 mm) inside the cladding tube (with an outer diameter of 6 mm and inner diameter of 4 mm) in exact orthogonal positions, using a modified chemical vapor deposition (MCVD) glass working lathe and one hydrogen-oxygen torch. The temperature was adjusted so that a lateral homogenous peripheral sintering was achieved. An elliptical deformation of the outer cladding tube and collapse was prevented by selecting a preferably low temperature and short lateral heating zone (ca. 1 cm). The preform was drawn to the final fiber by pressurized drawing with a constant temperature. The pressure inside the preform was varied between 1000 Pa and 3000 Pa above atmospheric pressure to shift the cavity size inside the fiber. It was drawn to a diameter of 125  $\mu\text{m}$  and coated with single layer UV acrylate. The effect of increasing the pressure on the cavity cross section is shown in Fig. 1 [17].

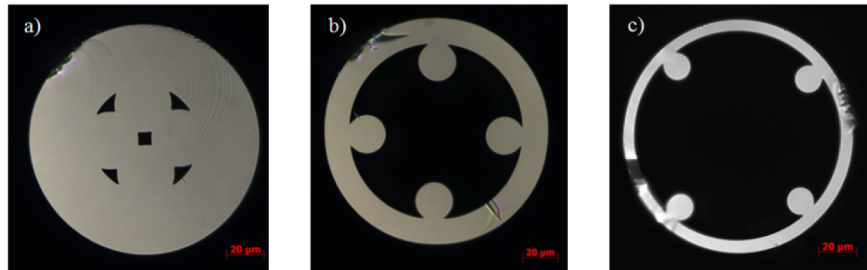


Fig. 1. Micrographs of drawn fibers, varying the pressure during fiber drawing: (a)  $p = 1000$  Pa, (b)  $p = 2300$  Pa and (c)  $p = 3000$  Pa.

From the different silica tubes drawn, the one shown in Fig. 1(b) was used as the sensing element. The silica tube presented a cladding with a thickness of  $\sim 14$   $\mu\text{m}$ , a hollow core and four small rods positioned in diametrically opposite directions. Each rod has a diameter of  $\sim 20$   $\mu\text{m}$  and has a reinforcement effect in the structure. This matter will be discussed later on this paper.

The Fabry-Perot (FP) cavity shown in Fig. 2 was produced by splicing a short section of the silica tube between two sections of standard single mode fiber (SMF). In order to prevent the collapsing of the structure in the splice region, both splices were done in the manual program of the splice machine (Fujikura FSM-60S) and the fibers were placed with a lateral offset regarding the electric arc discharge area. Thus, the discharge was mainly produced in the SMF region. Notice that the FP cavity did not present coating, as it was removed during the fabrication process. The sensors were easy to manufacture and reproducible. The strain and temperature measurements were performed in reflection, by connecting the broadband optical source, the sensing head and the optical spectrum analyzer to an optical circulator, according to the scheme in Fig. 2. The optical source had a bandwidth of 100 nm, centered at 1570 nm and the measurements were done with a resolution of 0.02 nm.

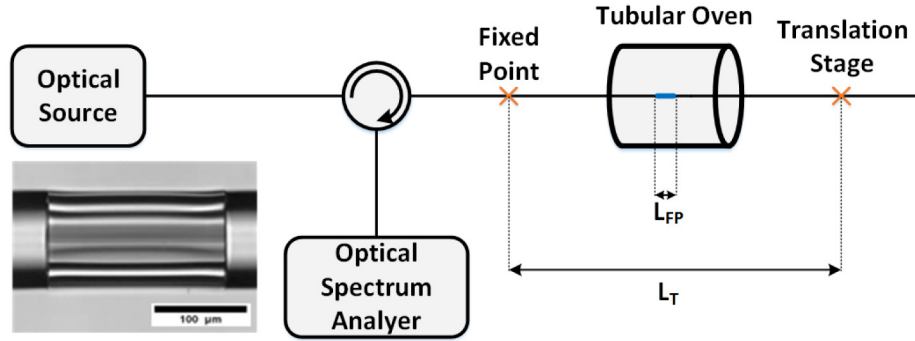


Fig. 2. Scheme of the experimental setup. A microscope photograph of one FP cavity is also shown.

Several sensing heads were produced, with different cavity lengths. The spectrum of each sensor, presented in Fig. 3, is the result of a two wave interferometer. The two reflections occur at the interfaces between SMF and the silica tube. The effective refractive index,  $n_{eff}$  was estimated according to Eq. (1):

$$L_{FP} = \lambda_1 \lambda_2 / (2n_{eff} \Delta\lambda) \quad (1)$$

where  $L_{FP}$  corresponds to the length of the FP cavity,  $\lambda_1$  and  $\lambda_2$  are the wavelengths of two adjacent fringes and  $\Delta\lambda = \lambda_2 - \lambda_1$  is the free spectral range. The value obtained for the  $n_{eff}$  was of  $\sim 1.00$ , which means that all light travels inside the hollow core.

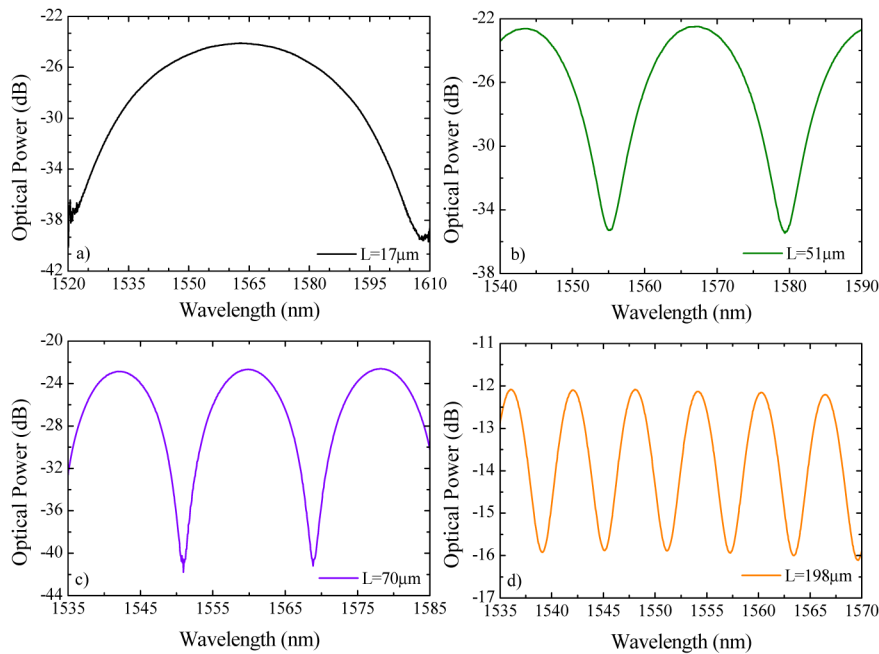


Fig. 3. Spectra of the four FP cavity sensors with lengths of (a) 17  $\mu\text{m}$ , (b) 51  $\mu\text{m}$ , (c) 70  $\mu\text{m}$  and (d) 198  $\mu\text{m}$ .

In a first stage, the sensing heads were attached to a translation stage with a resolution of 0.01 mm and strain measurements were performed at room temperature. The experimental data, shown in Fig. 4(a), exhibit a linear behavior of the wavelength shift with the applied

strain. As expected, the sensitivity to strain depends on the cavity length: smaller cavities translate into more sensitive devices. According to ref [18], the response of the sensor depends not only on the FP cavity length, but also on the total length over which strain is applied. In this study, the total length,  $L_T$ , was of 73.5 cm and it was kept constant for all the strain measurements. Sensitivities of 13.9 pm/ $\mu\epsilon$ , 6.0 pm/ $\mu\epsilon$ , 4.6 pm/ $\mu\epsilon$  and 3.5 pm/ $\mu\epsilon$  were respectively obtained for the 17  $\mu\text{m}$ , 51  $\mu\text{m}$ , 70  $\mu\text{m}$  and 198  $\mu\text{m}$  long sensing heads. The non-linear behavior of the strain sensitivity with the cavity length has been described in detail in [18].

The 198  $\mu\text{m}$  long sensing head was placed inside a tubular oven, with the FP cavity positioned at its center. The fiber was kept straight but loose, without any tension. The sensor was subjected to a temperature variation of  $\sim 900^\circ\text{C}$  and its response is shown in Fig. 4(b). The experimental data was well adjusted to a linear fitting and a sensitivity of 0.85 pm/ $^\circ\text{C}$  was attained, which indicates that this sensor has a cross sensitivity of  $\sim 0.18 \mu\epsilon/^\circ\text{C}$ . Besides, for this sensor thermal sensitivity, and considering a wavelength of 1547.14 nm, one gets  $\Delta L/L = 5.49 \times 10^{-7}/^\circ\text{C}$ , which is in good agreement with the silica thermal expansion coefficient presented in the literature, of  $5.5 \times 10^{-7}/^\circ\text{C}$  [14].

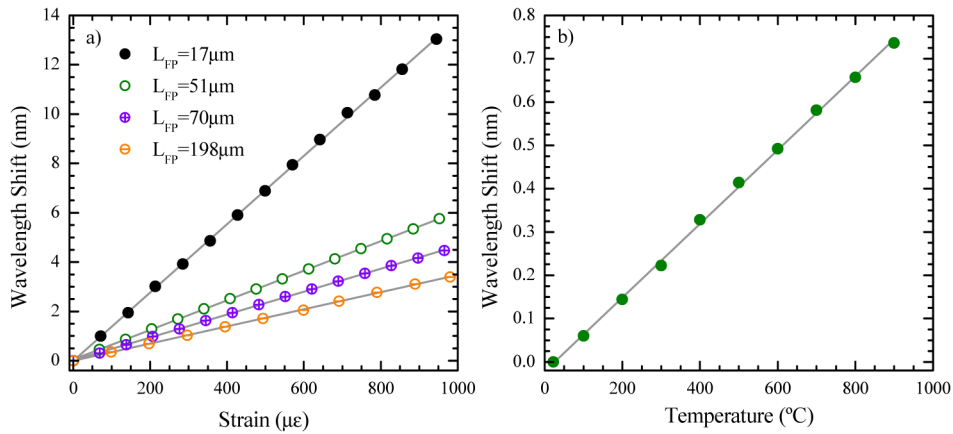


Fig. 4. (a) FP cavity sensors response to the applied strain. (b) The 198  $\mu\text{m}$  long FP cavity sensor response to temperature.

Since this FP cavity presents such low temperature sensitivity, it is worthwhile to study its behavior when strain is applied in extreme temperature conditions. The 70  $\mu\text{m}$  long sensing head was placed in a tubular oven and on the outside the fiber was fixed to a translation stage. The temperature was increased from room temperature ( $\sim 22^\circ\text{C}$ ) to  $750^\circ\text{C}$  in steps of  $150^\circ\text{C}$ . From  $750^\circ\text{C}$  to  $900^\circ\text{C}$  the steps were of  $50^\circ\text{C}$ . At each temperature step the setup was stable for 30 minutes and the fiber was kept straight with a slight tension. After that time, strain measurements were done, by increasing the tension in the fiber up to  $1000 \mu\epsilon$  (up curves in Fig. 5), and decreasing it back to its initial state (down curves in Fig. 5). Until  $600^\circ\text{C}$ , the behavior was nearly the same and the sensitivities obtained when increasing strain were similar as when decreasing it. However, from  $750^\circ\text{C}$  on, the sensor showed higher sensitivity as strain increased, indicating that such high temperature has the effect of reducing the Young modulus of the silica tube, also associated with a certain level of induced plasticity, as indicated by the fact interferometric fringes do not return to the original wavelength values when the strain is decreased to zero (it is observed a red shift of  $\sim 1 \text{ nm}$ , resulting from this a reduction of the strain sensitivity during the step of diminishing the applied tension).

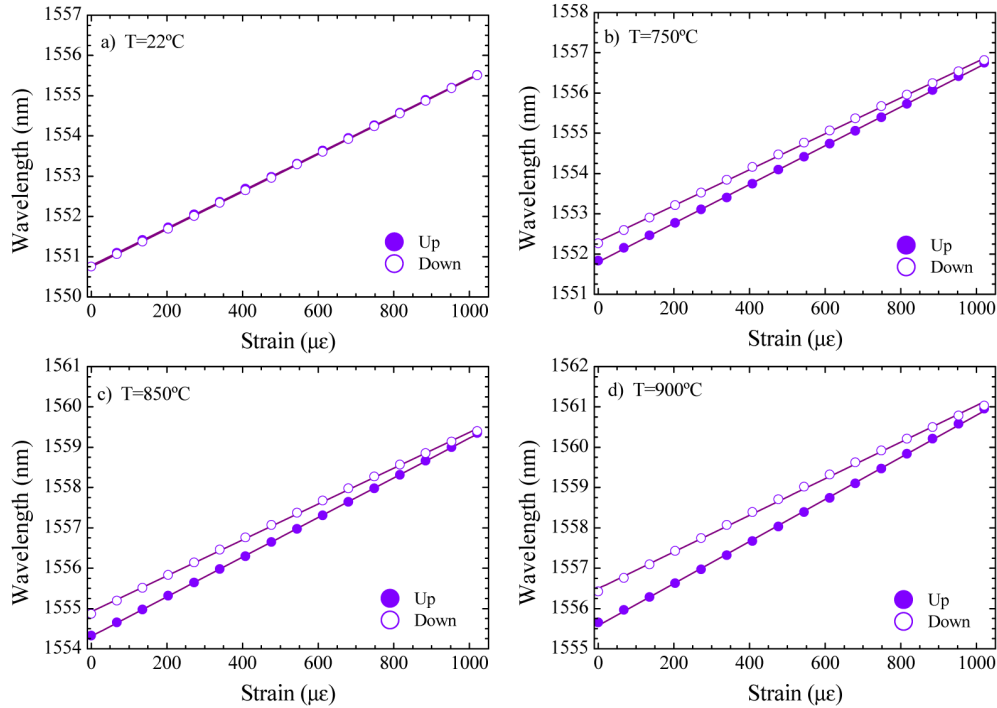


Fig. 5. Response of the 70  $\mu\text{m}$  long FP cavity to the applied strain at (a) room temperature, (b) 750  $^{\circ}\text{C}$ , (c) 850  $^{\circ}\text{C}$  and (d) 900  $^{\circ}\text{C}$ . Up and down stand for increasing and decreasing the applied strain, respectively.

The annealing effect was studied by subjecting the 51  $\mu\text{m}$  long sensing head to a temperature of 900  $^{\circ}\text{C}$  for 7 hours (see Fig. 6). There was a total wavelength shift of 4.4 nm throughout this period of time. In the first 40 minutes the variation was of  $\sim 0.1$  nm/min. After that time, the wavelength shift became slower and from 4 hours to 7 hours the change was of  $\sim 3$  pm/min. The oven was then switched off and cooled down until it reached room temperature.

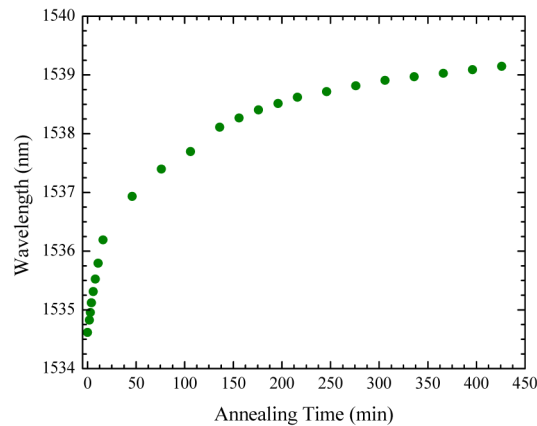


Fig. 6. Wavelength shift of the 51  $\mu\text{m}$  long FP cavity for an annealing temperature of 900  $^{\circ}\text{C}$ .

The same procedure as for the 70  $\mu\text{m}$  long sensing head was then carried on for this FP cavity, and the results are depicted in Fig. 7. In this case, the difference between increasing

and decreasing the applied strain at high temperatures was not as notorious as in the previous experiment. The small difference at 900 °C can be due to the fact that the annealing was not fully performed.

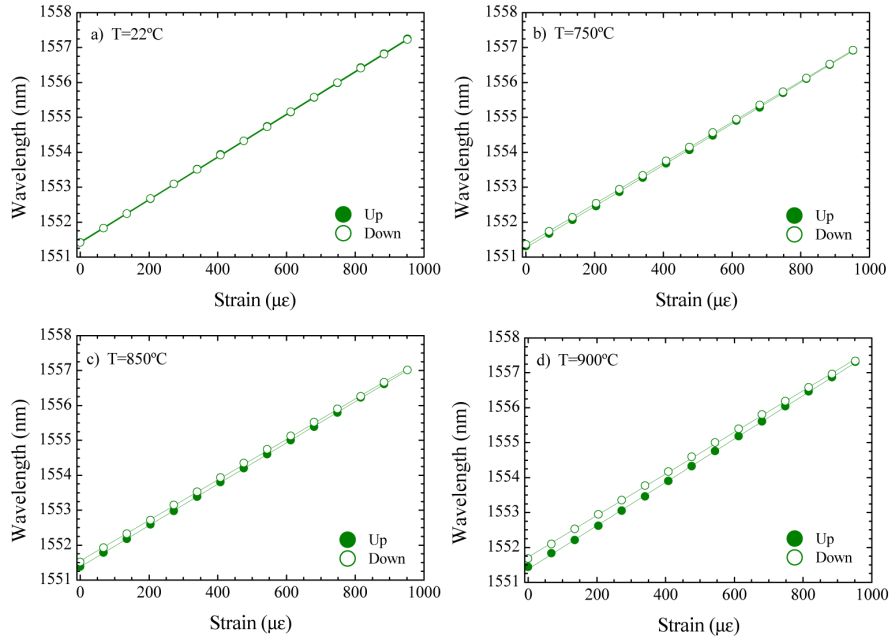


Fig. 7. Response of the 51  $\mu\text{m}$  long FP cavity to the applied strain at (a) room temperature, (b) 750 °C, (c) 850 °C and (d) 900 °C, after an annealing period of 7 hours, at 900 °C. Up and Down stand for increasing and decreasing the applied strain.

It is also interesting to observe how the strain sensitivity changes with temperature. In all the sensors tested the strain sensitivity decreased as temperature increased up to 600 °C, increasing again afterwards (Fig. 8). This effect can be attributed to two reasons: the non-linear variation of the thermal expansion of silica as temperature arises [19], as well as the variation of the photoelastic constant of the silica tube with this parameter. The photoelastic constant is essentially determined by the Pockel's coefficient,  $p_{12}$ , which exhibits a maximum at 600 °C [20], translating into a minimum in the strain sensitivity. Nevertheless, the difference between applying strain or reduce it is much more significant when no annealing occurred.

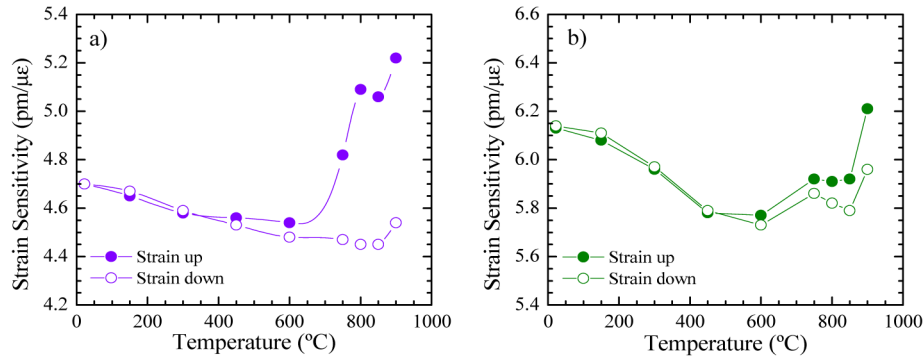


Fig. 8. Dependence of the strain sensitivity at different temperatures (a) without annealing and (b) with annealing.

The silica tube design used in this work proved to be mechanically stable in harsh conditions, such as strain at extreme temperatures. Its behavior was also compared with a FP cavity based on a pure silica tube fabricated under the same conditions. In this case, the silica tube had a hollow core diameter of  $\sim 57 \mu\text{m}$  with a total cross-section area of  $\sim 2552 \mu\text{m}^2$ . Regarding the new design, its hollow cross section area was of  $\sim 5981 \mu\text{m}^2$ . Two sensors, fabricated with a length of  $\sim 1.2 \text{ mm}$ , were subjected to strain until rupture. The sensor based on the silica tube without rods was able to measure strain up to  $1500 \mu\epsilon$ , with a linear sensitivity of  $2.18 \text{ pm}/\mu\epsilon$ . Regarding the sensor with the new silica tube design, it was possible to measure strain up to  $2500 \mu\epsilon$  with a linear sensitivity of  $3.39 \text{ pm}/\mu\epsilon$ . Due to the presence of the internal rods in this design it is not possible to perform direct comparisons of its mechanical characteristics with those associated with a standard silica tube. Anyway, the relevant topic to emphasize is that the new design shows favorable sensing properties both in what concerns strain sensitivity and mechanical resilience, indicating its adequacy for application in harsh environments.

### 3. Conclusions

A Fabry-Perot sensor was proposed to measure strain at high temperatures. The cavity was formed by splicing a new advanced silica tube between two sections of standard single mode optical fiber. The new hollow core silica tube presents a thin cladding supported on its inside by four small rods with diametrically opposed positions. The presence of the four rods ensures a higher mechanical stability besides a higher sensitivity to strain, when compared to a traditional silica tube. Different sensors were produced by varying the cavity lengths, and subjected to strain and temperature variations. The  $17 \mu\text{m}$  long sensor presented a sensitivity of  $13.9 \text{ pm}/\mu\epsilon$ . The sensitivity to temperature of this configuration was below  $1 \text{ pm}/^\circ\text{C}$ , with the thermal expansion of silica being the dominant effect. Since this configuration presented low sensitivity to temperature, it was considered to be a good candidate to measure strain at extreme temperatures. However, when strain was applied at temperatures above  $750^\circ\text{C}$ , the sensitivity increased as the fiber was being tensioned. When the fiber returned to its initial state, without strain applied, the sensitivity decreased to a value similar to the one found at lower temperatures. This difference was reduced through thermal annealing before subjecting the sensing head to strain at extreme conditions. Furthermore, the strain sensitivity decreased as temperature increased up to  $600^\circ\text{C}$ , where it reached a minimum. Above  $750^\circ\text{C}$  it was observed an increase of the strain sensitivity.

### Acknowledgments

This work was supported by FCT – Fundação para a Ciência e Tecnologia (Portuguese Foundation for Science and Technology) under the grant SFRH / BD / 76965 / 2011. The authors also thank to Portuguese national funds, through a bilateral cooperation between the Portuguese and the German academic exchange service funding agency, FCT/DAAD.